

Mass and transverse momentum dependence of dielectron production in $p + d$ and $p + p$ collisions at 4.9 GeV

H. Z. Huang,^{1,*} S. Beedoe,^{2,†} M. Bougheb,³ J. Cailiu,^{1,‡} J. Carroll,²
 T. Hallman,^{4,§} L. Heilbronn,¹ G. Igo,² P. Kirk,⁵ G. Krebs,¹
 A. Letessier-Selvon,^{1,||} B. Luttrell,¹ F. Manso,³ L. Madansky,⁴ H. S. Matis,¹
 D. Miller,⁶ J. Miller,¹ C. Naudet,¹ R. J. Porter,¹ G. Roche,^{1,3} L. S. Schroeder,¹
 P. A. Seidl,¹ Z. F. Wang,⁵ R. Welsh,⁴ W. K. Wilson,¹ and A. Yegneswaran⁷

(DLS Collaboration)

¹Lawrence Berkeley Laboratory, University of California, Berkeley, California 94720

²University of California at Los Angeles, California 90024

³Université Blaise Pascal/IN2P3, 63177 Aubière cedex, France

⁴The Johns Hopkins University, Baltimore, Maryland 21218

⁵Louisiana State University, Baton Rouge, Louisiana 70803

⁶Northwestern University, Evanston, Illinois 60201

⁷Continuous Electron Beam Accelerator Facility, Newport News, Virginia 23606

(Received 7 June 1993)

Dielectron production in $p + d$ and $p + p$ collisions at the beam kinetic energy of 4.9 GeV has been measured with the Dilepton Spectrometer DLS. Features of the dielectron cross section have been studied with cuts on the mass and transverse momentum of the pairs. The spectra for several regions of phase space are presented as a function of the pair mass and transverse momentum.

PACS number(s): 25.40.Ve, 13.75.Cs, 21.65.+f

I. INTRODUCTION

Production of dileptons with masses below 1 GeV/ c^2 in nuclear collisions has been of considerable interest for several decades. Early measurements for hadron-nucleon and hadron-nucleus collisions at beam energies of 10–20 GeV to a few hundred GeV observed a large yield of low mass dileptons, which could not be explained by extrapolation of Drell-Yan processes or by Dalitz and direct decays of mesons and resonances [1]. Two major classes of models, soft-parton annihilation [2] and virtual pion annihilation [3], were proposed to explain the observed dilepton yield. Although two fundamentally different mechanisms (parton and meson annihilations) were used, such models were not distinguishable using available experimental results. In addition, a few experiments in the same beam energy region measured no significant excess of low mass dileptons over hadronic decay sources [4–6]. These ambiguities in both theoretical understanding and experimental measurements have not been resolved.

The production of direct leptons as a function of in-

cident beam energy also raised questions regarding possible threshold behavior in production mechanisms. An experiment measured no signal of direct leptons in $p + p$ collisions at beam energy of 0.8 GeV [7], while many experiments consistently observed signals of direct dileptons in nuclear collisions at beam energies above 10 GeV [1]. Here “direct” historically meant those photons and leptons that are not decay products of produced particles and resonances, although these products (such as Dalitz decay of Δ 's) can also be of interest. The Dilepton Spectrometer (DLS) collaboration at the Bevalac (Lawrence Berkeley Laboratory) was initiated to bridge the gap in beam energy for the lepton measurements. To date the DLS has established dielectron (electron-positron) signals in collisions of $p + \text{Be}$ at beam kinetic energies (E_k) of 1.0, 2.1, and 4.9 GeV. Furthermore, the DLS has measured dielectron production in $\text{Ca} + \text{Ca}$ ($E_k/A=1.0$ and 2.1 GeV) and $\text{Nb} + \text{Nb}$ ($E_k/A=1.0$ GeV) collisions [8–10].

Because photons and leptons, unlike hadrons, suffer little final state interactions, they can probe the interior of nucleus-nucleus collisions, where a large volume of dense and hot nuclear matter can be formed. Although the original expectation [11] that dielectrons could be used to study the pionic self-energies in dense nuclear matter was modified substantially when the form factor of Δ and the correction of the pion-pion annihilation vertex were included [12], dielectron production in the ρ mass region can still probe the nuclear medium effect on pion dynamics [13]. Early theoretical studies of dielectron production in nucleus-nucleus and proton-nucleus collisions at the Bevalac energies indicated that the dominant dielectron production mechanisms were bremsstrahlung of proton-neutron scattering, Dalitz decay of Δ 's, and pion-

*Present address: Purdue University, West Lafayette, IN 47907.

†Present address: Hampton University, Hampton, VA 23668.

‡Present address: Beijing High Energy Institute, Beijing, China.

§Present address: University of California at Los Angeles, CA 90024.

||Present address: Université de Paris VI et VII, LPNHE, 75252 Paris Cedex 05, France.

pion annihilations [13]. More recently, the Dalitz decay of η was found to contribute significantly to the dielectron yield in proton-nucleus and nucleus-nucleus collisions [5, 6, 14]. Among the various sources of dileptons, both pion-pion annihilation and Dalitz decay of the Δ are considered promising probes of dense nuclear matter. The yield of dielectrons from pion-pion annihilation depends on the equation of state and pion dynamics; the dielectrons from the Dalitz decay of Δ 's can reflect the evolution of nucleon resonances during the collision, thus providing a means of studying the collision dynamics.

In order to study the time evolution of the colliding nuclei and the equation of state of nuclear matter using dileptons, we have to understand the dilepton production mechanisms in elementary nucleon-nucleon collisions. The DLS collaboration has undertaken a program to measure dielectron production in $p+d$ and $p+p$ collisions at the beam energy ranging from 1.0 to 4.9 GeV. Our previous results [15] indicated that the expectation from current $p+n$ bremsstrahlung calculations failed to explain the observed relative yield of dielectrons from $p+d$ and $p+p$ collisions at the beam energy of 4.9 GeV. Furthermore, the estimated total contribution from hadronic decays of η , Δ , ρ , and ω was not able to account for the yield from $p+p$ collisions. Our recent study [16] found that the ratio of dielectron yield for $p+d$ to that for $p+p$ collisions decreases with beam energy, being about nine for E_k of 1 GeV, and two for $2.1 < E_k < 4.9$ GeV. The relatively large ratio at 1 GeV may be consistent with the assumption that $p+n$ bremsstrahlung is a dominant mechanism which is not present in $p+p$ collisions, but its steep decrease to about two could be indicative of the onset of production processes, perhaps with a hadron-like origin, that are similar in both $p+n$ and $p+p$ collisions.

The number of dielectron pairs from this data set of $p+d$ and $p+p$ collisions at 4.9 GeV is close to 10^4 , an increase of almost two orders of magnitude in statistics over previous dielectron measurements. In this paper, we explore the mass and transverse momentum dependence of dielectron production in these collisions. Our extensive data will provide better constraints on theoretical understanding of dielectron production mechanisms, which should also shed light on the deficiencies of existing models. The paper is arranged as follows. In Sec. II, we describe the experimental apparatus, acceptance, and analysis. The experimental results and discussion follow in Sec. III, and we summarize in Sec. IV.

II. EXPERIMENTAL APPARATUS, ACCEPTANCE, AND ANALYSIS

Figure 1 shows a schematic view of the Dilepton Spectrometer (DLS), which consists of two identical magnetic spectrometer arms. Each arm has one Čerenkov array, one scintillator array, and one drift chamber in front of the dipole magnet, and two drift chambers, one Čerenkov array, and one scintillator array after the magnet. The list of detectors is ordered according to distance from the target (which is about 89 cm for the front Čerenkov array and about 360 cm for the rear scintillator array). Two

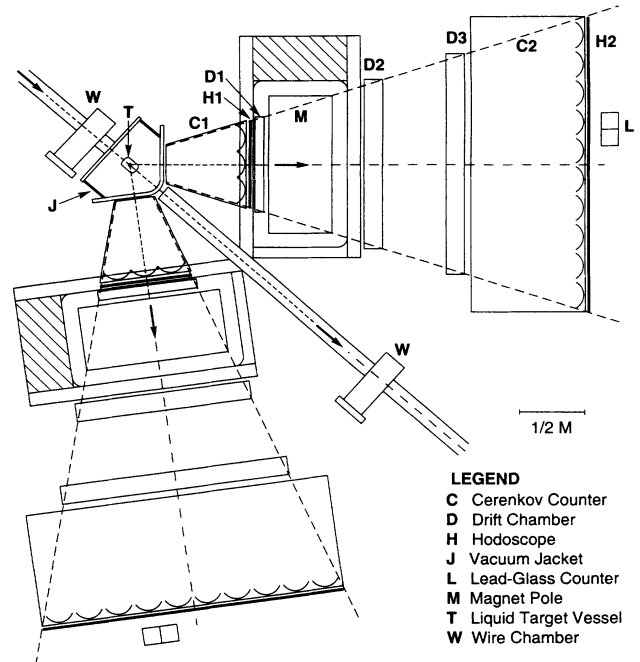


FIG. 1. Schematic top view of the Dilepton Spectrometer (DLS). Note the scattering chamber has been replaced by the liquid target system.

wire chambers downstream of the apparatus are used to monitor beam tuning on a spill-by-spill basis. Details of the DLS have been described elsewhere [17].

The cylindrical target vessel, which replaced the solid target holder that was used in the previous measurements, is made of 0.127-mm-thick Kapton with a diameter of about 7.6 cm and a length of 12.7 cm. Ten layers of aluminized Mylar, each about 0.00635-mm-thick, surrounded the target except a few cm^2 near the beam entrance and exit. This vessel is contained in a vacuum jacket which is directly connected to the upstream beam pipe. The vacuum jacket has one wide window made of 0.889-mm-thick Kapton in the beam line downstream of the target; it also covers the apertures of both spectrometer arms. The typical proton beam at the Bevalac is about 1 cm in diameter. With this target system, we measured a ratio of dielectrons for full target to that for empty target of 20 for $p+d$ and 10 for $p+p$ collisions. The empty-target contribution was subtracted in the analysis.

The Čerenkov and scintillator detectors were calibrated at the beginning of each major run. The hadron rejection factor of each arm was at the level of a few times 10^{-4} . The detection efficiency of electrons for Čerenkov counters, and the detection efficiency of charged particles for scintillator counters, were essentially 100%. Data were taken with dielectron triggers which corresponded to eightfold coincidence of responses from all scintillator and Čerenkov counters.

The response of each detector was described in a simulation package using the GEANT library [18]. The momentum resolution obtained from the GEANT simulations of $p+p$ elastic scattering is consistent with that observed in the detector for collisions at 1.0 and 1.26

GeV, and the DLS measurements of these cross sections [19] are in agreement with earlier data [20].

The acceptance for dielectron pairs was computed using the simulation package, including effects of multiple scattering and electron bremsstrahlung. Each dielectron pair was uniquely specified by six variables—mass, transverse momentum, rapidity, and azimuthal angle (ϕ) in the beam frame, and azimuthal and polar angles of the decay in the pair center-of-mass (c.m.) frame. We have assumed an azimuthal symmetry in ϕ and an isotropic decay in the c.m. frame of the decaying virtual photon, and computed a three-dimensional acceptance table as a function of the dielectron mass (M), the transverse momentum (p_t), and the laboratory rapidity (y). In generating the table, we have accepted $> 3 \times 10^6$ dielectrons corresponding to more than 10^9 generated events. We also studied the effect of the assumption of isotropic decay of the virtual photons and found that there is a variation of about 15% in the acceptance, due to different angular distributions ($d\sigma/d\Omega \sim 1, 1+\cos^2\theta, 1+\sin^2\theta$). This variation is less than the systematic errors of the data due to detector effects.

The binning of the acceptance table was chosen to be 0.025 GeV/ c^2 in M , 0.05 GeV/ c in p_t , and 0.05 in y . These bins led to a significant improvement in accuracy, compared to the previous acceptance table, which had bins of 0.05 GeV/ c^2 in M , 0.1 GeV/ c in p_t , and 0.2 in y [9]. The small bins in acceptance allowed us to better define the fiducial volume of the acceptance, which was defined by a cut on the minimum acceptance of 0.001 (or maximum weight of 1000 for pairs in the calculation of the cross section). In addition, we required M within 0.05–1.0 GeV/ c^2 , p_t within 0.0–1.0 GeV/ c , and y within 0.45–1.95. For most measured pairs, the acceptance was calculated by interpolating between the grid points where the acceptance table was generated. For data at the edge of the fiducial region, where no interpolation could be performed, the acceptance of the pair was taken to be that of the nearest grid point.

Most of the background in our measurement comes from combinatorial dielectrons from photon conversions and Dalitz decays. Improvements have been made in the analysis to reject these dielectron pairs without a significant multiplicity bias. In analyses of earlier data we imposed a maximum allowed value on the energy deposition of charged particles (ADC) in the front scintillator array element, to reject events generated by the conversion of real photons and the Dalitz decay of neutral pions, where the opening angle of two outgoing electrons are small. That analysis cut, however, introduced a bias against events in which an electron and a hadron traversed a single front scintillator element, which produced a multiplicity-dependent efficiency. Extensive simulations were needed to obtain the efficiency due to this cut. This analysis procedure allowed us to obtain a clean sample of dielectron events, and led to the unambiguous establishment of dielectron signals in nucleus-nucleus collisions with a potential compromise on the accuracy of the absolute normalization.

For the current $p+d$ and $p+p$ data set, we have cut on the ADC values of the front Čerenkov counters in-

stead. Because the total responses from hadrons in each Čerenkov element due to scintillation processes are very small compared to these from electrons for $p+d$ and $p+p$ collisions, this Čerenkov ADC cut proved to be efficient in rejecting those events with dielectrons in one arm, either from Dalitz decay of pions or from photon conversions. The maximum allowed value of the Čerenkov ADC was set to be twice the response of the detector to a single electron traversal. In addition, we required that the leptons, one only per arm, must have a separation of arrival time, measured by the front scintillator counters in each spectrometer arm, less than 5 ns.

To obtain the combinatorial background, we have measured electron-electron and positron-positron pairs (same-sign pairs) with all possible bending configurations in the two spectrometer arms. In previous analyses, the combinatorial background was removed by simply subtracting the same-sign pairs (SS) from the opposite-sign pairs (OS). This subtraction scheme is valid when the numbers and kinematics of electrons and positrons in the background are the same. In our current data set, we observed 30% more electron-electron than positron-positron pairs, mostly in the forward direction (this excess of electrons is consistent with that from Compton scattering of photons in the target). Because of the differences in the kinematics and the yield between electrons and positrons, the simple subtraction scheme is not exactly valid. We constructed a combinatorial electron-positron background (OSBK) by randomly selecting an electron and a positron each from the sample of same-sign pairs for each bending configuration (determined by the charge of the particle and the field polarity). The number of the background pairs was normalized to the square root of the product of the number of electron-electron and positron-positron pairs. The uncertainties in the subtraction scheme lead to an estimated error in the cross section of up to 20% for masses below 0.3 GeV/ c^2 , negligible for high masses.

Our tracking software, for the hardware plane efficiency of about $(95 \pm 5)\%$ for drift chambers and the overall hit position resolution about 1 mm on each plane, had an efficiency of about 95% for each arm. For high momentum particles, the tracking misidentified the charge at the level of a few percent, due to finite chamber resolutions. This charge misidentification introduced a systematic error of about 25% for masses greater than 0.8 GeV/ c^2 . Thus systematic errors which could modify the shape of the dielectron spectrum are limited to the mass regions below 0.3 GeV/ c^2 and above 0.8 GeV/ c^2 .

The systematic error on the normalization was estimated to be 40%, mostly from the uncertainties of the trigger efficiency. High single-particle rates in trigger elements produced significant inefficiencies in the trigger electronics [21]. The trigger efficiency was obtained by studying the dielectron yield as a function of beam intensity. The overall detection efficiencies for dielectrons are 43% for $p+d$, and 48% for $p+p$ collisions.

III. RESULTS AND DISCUSSIONS

Figure 2 shows the cross section of dielectron production as a function of the pair mass for $p+d$ and $p+p$

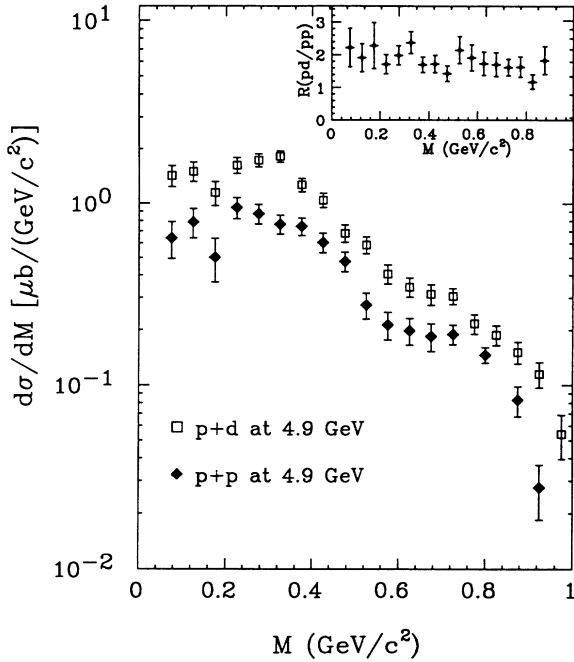


FIG. 2. $d\sigma/dM$ for $p+d$ and $p+p$ collisions at the beam kinetic energy of 4.9 GeV, where errors are statistical only. Events with masses below $0.15 \text{ GeV}/c^2$ are mostly from the Dalitz decay of π^0 . The inserted plot shows the ratio of dielectron production for $p+d$ to that for $p+p$ collisions as a function of dielectron masses.

collisions at the beam kinetic energy of 4.9 GeV. Both exhibit similar features: a shoulder at the ρ - ω mass region and a peak structure near the mass of $0.3 \text{ GeV}/c^2$. The cross section below $0.15 \text{ GeV}/c^2$ is essentially due to the Dalitz decay of neutral pions. The inserted plot shows the ratio of the cross section for $p+d$ to that for $p+p$ collisions. The ratio of integrated cross section for masses above $0.2 \text{ GeV}/c^2$ is 1.9 ± 0.1 , and the ratio of yield without acceptance correction is 1.92 ± 0.06 . The errors shown are statistical only, and the systematic error on the ratios was estimated to be about 20% [15]. We pointed out in Ref. [15] that the similarity of the shape and the value of the ratio for $p+d$ and $p+p$ collisions are in disagreement with the expectation of theoretical models [13]. In these model calculations, dielectrons at this beam energy came mostly from bremsstrahlung of proton-neutron scattering, which led to the prediction of a large ratio of dielectron production in $p+d$ to that in $p+p$ collisions.

Although the similarity in the dielectron mass spectra and the ratio of about two are indicative of hadron-like origins for the dielectron production, our GEANT simulation of the total dielectron contribution from hadronic decays of η , Δ , ρ , and ω failed to account for the observed yield of dielectrons by a factor of 3–4 [15]. The hadron production cross sections used in the simulation were estimated from a few measurements of exclusive channels near our beam energy. However, we also note that recent results from the HELIOS experiment [6] showed that within errors of 30% the dilepton production in $p+\text{Be}$

collisions at a beam energy of 450 GeV can all be explained by the Dalitz decay of η and ω 's, where a large production cross section for η (by a factor of 3 larger than previous estimates) was measured in their apparatus. A measurement of the production cross section for η at our beam energy is of determinative importance, especially because the observed dielectron yield cannot be accounted for, even when using an upper limit of the η cross section estimated from bubble-chamber data.

The shape of the mass spectra near $0.3 \text{ GeV}/c^2$ has also been an interesting topic [11, 12], because it may be indicative of annihilation processes of produced pions where a threshold is due to the masses of two pions [9, 22]. Attempts to use the KSS [23] and soft-parton annihilation [2] models to fit the $p+\text{Be}$ data at 4.9 GeV were not successful [9]. However, it is not clear that pion-pion annihilation would play an important role in $p+p$ collisions because of low multiplicities. We also note that the calculation for bremsstrahlung of $p+n$ scattering [13, 24] either failed to yield any peak structure, or yielded a peak at masses lower than $0.3 \text{ GeV}/c^2$. The Dalitz decay of η [15], though too small to match in magnitude, did yield a structure similar to the observed shape of the spectra. We shall comment on the nature of this peak structure again later in this section.

Figure 3 shows the transverse momentum distribution of dielectrons for $p+d$ and $p+p$ collisions for all pairs with masses between 0.05 and $1.0 \text{ GeV}/c^2$ within DLS acceptance. Both exhibit an approximately exponential behavior with an enhancement in the lowest p_t bins. This enhancement is largely due to dielectron pairs from the Dalitz decay of pions. Because of the low mass of these pairs, any pair that can make it through the two spectrometer arms has a very small transverse momentum due to the DLS acceptance.

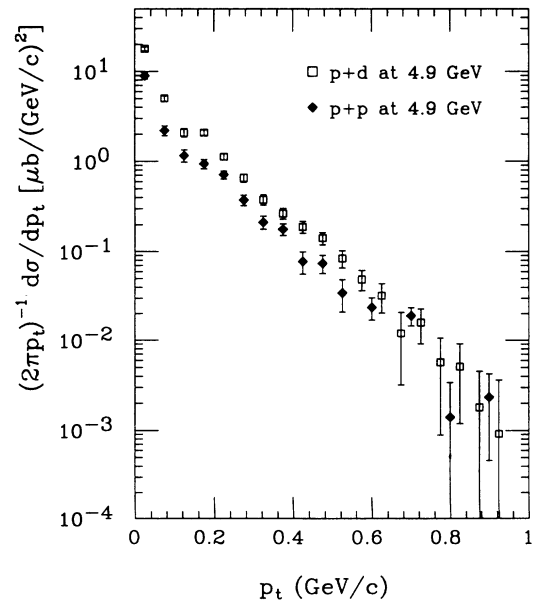


FIG. 3. $(\frac{1}{2\pi p_t})d\sigma/dp_t$ as a function of p_t for $p+d$ and $p+p$ collisions, containing all pairs within the DLS acceptance including those from Dalitz decay of π^0 .

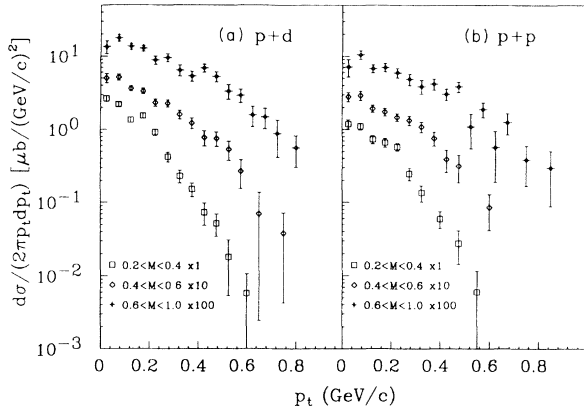


FIG. 4. $(\frac{1}{2\pi p_t})d\sigma/dp_t$ of dielectrons from $p+d$ (a) and $p+p$ (b) collisions as a function of p_t for dielectron mass of 0.2–0.4 GeV/ c^2 , 0.4–0.6 GeV/ c^2 , and 0.6–1.0 GeV/ c^2 , where the shown cross sections are scaled by 1, 10, and 100, respectively.

The unprecedented large number of pairs in this analysis, 10^4 , enabled us to study the dielectron production in detail with cuts on kinematic variables of M and p_t . For comparison, our previous study of $p+Be$ collisions by Letessier-Selvon *et al.* [9] contained about 500 pairs. The mass spectra of Fig. 2 were partitioned into three regions: an η -like region with mass 0.2–0.4 GeV/ c^2 , a medium mass region of 0.4–0.6 GeV/ c^2 , and a ρ - ω region of 0.6–1.0 GeV/ c^2 . Figures 4(a) and 4(b) show the p_t spectra of these three mass regions for $p+d$ and $p+p$ collisions, respectively. The p_t spectrum of dielectrons for both $p+d$ and $p+p$ collisions becomes flatter as the pair masses increase; no enhancement in the low p_t region is exhibited in any of these spectra.

In Figs. 5(a) and 5(b) we show the mass spectra of $p+d$ and $p+p$ collisions for p_t regions of 0.0–0.1 GeV/ c , 0.1–0.3 GeV/ c , and 0.3–1.0 GeV/ c . The shape of the spectra for $p+d$ and $p+p$ collisions with this cut also show striking similarity. The low mass cutoff for high p_t pairs is due to DLS acceptance, since low mass pairs with high transverse momentum tend to have small opening angles in the laboratory and cannot make it through both spectrometer arms.

Figures 5(a) and 5(b) show that the peak structure near 0.3 GeV/ c^2 in Fig. 2 results from a convolution of the DLS acceptance and the pair kinematics associated with dynamical production processes. The acceptance cutoff at the low mass end for high p_t pairs can lead to a bump structure in the mass spectra for pairs, including all p_t regions when the yields of comparable magnitude for different p_t regions are summed. This is the case for the Dalitz decays of the η , where a broad bump in the mass spectrum within the DLS acceptance was observed in the simulation, even though there is no peak present in the input cross sections [15]. However, for dy-

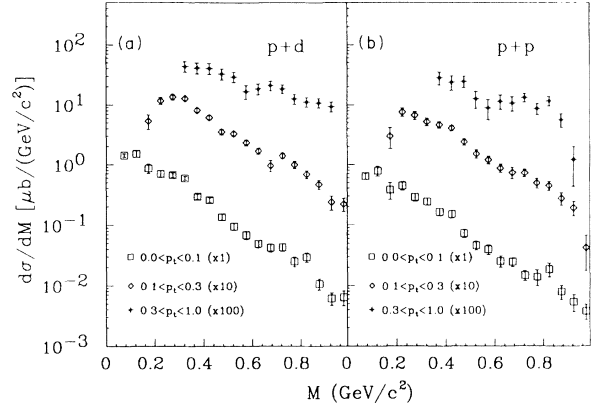


FIG. 5. $d\sigma/dM$ of dielectrons from $p+d$ (a) and $p+p$ (b) collisions as a function of pair mass for p_t of 0.0–0.1 GeV/ c , 0.1–0.3 GeV/ c and 0.3–1.0 GeV/ c , where the shown cross sections are scaled by 1, 10, and 100, respectively.

namical processes in which the pairs could be produced overwhelmingly at low p_t , the resulting mass spectrum would be essentially similar to the one for p_t between 0.0 and 0.1 GeV/ c without any structure. The KSS model and some calculations of $p+n$ bremsstrahlung should fall into this category.

IV. SUMMARY

We have measured dielectron production in $p+d$ and $p+p$ collisions at the beam kinetic energy of 4.9 GeV with large statistics. Spectra for various cuts in M and p_t are presented. The similarities in the spectra for both $p+d$ and $p+p$ collisions are indicative of the same dominant production processes in these collisions. The shape of the mass spectra was found to be strongly correlated to the transverse momentum dependence of the dielectron yield. This suggests that theoretical comparisons should be made in phase space of M and p_t simultaneously. These data should provide stringent constraints on theoretical understanding of the dielectron production in nucleon-nucleon collisions.

ACKNOWLEDGMENTS

This work was supported by the Director, Office of Energy Research, Office of High Energy and Nuclear Physics, Nuclear Physics Division of the U.S. Department of Energy under contracts No. DE-AC03-76SF00098, No. DE-FG03-88ER40424, No. DE-FG02-88ER40413, and No. DE-FG05-88ER40445. We thank W. G. Gong of LBL for useful discussions, Al Smith of LBL for calibrating ion-chambers, William Christie of Johns Hopkins for GEANT simulation work, and the Bevalac engineering and operations staff for their continued support of the DLS program.

- [1] L. M. Lederman, *Phys. Rep.* **26C**(4), 149 (1976); N. S. Craigie, *ibid.* **47**(1), 1 (1978).
 [2] J. D. Bjorken and H. Weisberg, *Phys. Rev. D* **13**, 1405 (1976); V. Cerny *et al.*, *ibid.* **24**, 652 (1981); P. Lichard

- and J. A. Thompson, *ibid.* **44**, 668 (1991).
 [3] T. Goldman *et al.*, *Phys. Rev. D* **20**, 619 (1979).
 [4] J. H. Cobb *et al.*, *Phys. Lett.* **78B**, 519 (1978).
 [5] A. Chilingarov *et al.*, *Nucl. Phys.* **B151**, 29 (1979).

- [6] U. Goerlach, Nucl. Phys. **A544**, 109c (1992).
- [7] A. Browman *et al.*, Phys. Rev. Lett. **37**, 246 (1976).
- [8] G. Roche *et al.*, Phys. Rev. Lett. **61**, 1069 (1988); G. Roche *et al.*, Phys. Lett. B **226**, 228 (1989); R. Welsh, Ph.D. thesis, The Johns Hopkins University (1992).
- [9] C. Naudet *et al.*, Phys. Rev. Lett. **62**, 2652 (1989); A. Letessier-Selvon *et al.*, Phys. Rev. C **40**, 1513 (1989).
- [10] S. Beedoe *et al.*, Phys. Rev. C **47**, 2840 (1993).
- [11] C. Gale and J. Kapusta, Phys. Rev. C **35**, 2107 (1987).
- [12] L. H. Xia *et al.*, Nucl. Phys. **A485**, 721 (1988); C. L. Korpa and S. Pratt, Phys. Rev. Lett. **64**, 1502 (1990); C. L. Korpa *et al.*, Phys. Lett. B **246**, 333 (1990).
- [13] C. Gale and J. Kapusta, Phys. Rev. C **40**, 2397 (1989); Gy Wolf *et al.*, Nucl. Phys. **A517**, 615 (1990); L. Xiong *et al.*, Phys. Rev. C **41**, R1355 (1990).
- [14] A. DePaoli *et al.*, Phys. Lett. B **219**, 194 (1989); Gy. Wolf *et al.*, *ibid.* **271**, 43 (1991); V. D. Toneev *et al.*, Report No. GSI-92-05 (1992); L. Winckelmann *et al.*, Phys. Lett. B **298**, 22 (1993).
- [15] H. Z. Huang *et al.*, Phys. Lett. B **297**, 233 (1992).
- [16] W. K. Wilson *et al.*, Phys. Lett. B **316**, 245 (1993).
- [17] A. Yegneswaran *et al.*, Nucl. Instrum. Methods Phys. Res. A **290**, 61 (1990).
- [18] R. Brun *et al.*, GEANT 3 User's Guide, CERN DD/EE/84-1.
- [19] H. Z. Huang *et al.*, Nuclear Science Division Annual Report No. LBL-30798.
- [20] K. A. Jenkins *et al.*, Phys. Rev. D **21**, 2445 (1980).
- [21] Our previous p+Be data may have an efficiency about 50% not corrected for. It is being investigated.
- [22] J. Kapusta and P. Lichard, Phys. Rev. C **40**, R1574 (1989).
- [23] K. Kinoshita, H. Satz, and D. Schildknecht, Phys. Rev. D **17**, 1834 (1978).
- [24] M. Schafer *et al.*, Phys. Lett. B **221**, 1 (1989).